Journal of Hazardous Materials B116 (2004) 239–248

Journal of Hazardous Materials

www.elsevier.com/locate/jhazmat

Decomposition of benzene in the RF plasma environment Part I. Formation of gaseous products and carbon depositions

Shun-I Shih, Ta-Chang Lin*, Minliang Shih

Department of Environmental Engineering, National Cheng Kung University, Tainan 70101, Taiwan

Received 5 February 2004; received in revised form 8 September 2004; accepted 10 September 2004

Abstract

This study employed radio-frequency (RF) plasma for decomposing benzene (C_6H_6) gas, and examined both gaseous products and solid depositions after reaction. The reactants and products were analyzed mainly by using both an on-line Fourier transform infrared (FT-IR) spectrometer and a gas chromatography. The analyses for solid deposition included electron spectroscopy for chemical analysis (ESCA), element analysis and heat value analysis. The C_2H_2, C_2H_4, C_2H_6, CH_4, CO_2 and CO were detected and discussed. The analytical results demonstrate that in the C_6H_6/Ar plasma, C_2H_2 is the sole gaseous product being detected. The fraction of total carbon input converted into C_2H_2 ($Y_{C_2H_2}$) increased with increasing C_6H_6 feed concentration, but decreased with increasing input power. In the C_6H_6/H_2/Ar system, besides C_2H_2, CH_4, C_2H_4 and C_2H_6 were also detected, and their yields increased with increasing H_2/C_6H_6 ratio. The above results indicated that the addition of H_2 (auxiliary gas) achieves the benefit of creating hydrogen-rich species like CH_4, C_2H_4 and C_2H_6. In the C_6H_6/O_2/Ar system, C_6H_6 could be totally oxidized into CO_2, CO and H_2O, and no measurable phenol was found. Analyses of solid depositions revealed that the carbon depositions were similar to those of Anthracite. The carbon deposition has a heat value of 7000 kcal/kg. Additionally, the possible reaction pathways were also built up and discussed.

Keywords: Radio-frequency; Plasma; Benzene (C_6H_6); Decomposition; Deposition

1. Introduction

Numerous types of plasma can be used to destroy C_6H_6 [1–6]. Non-thermal plasma, which has low energy requirements has been demonstrated to be an effective process for decomposing inorganic or organic air pollutants, leading to high destruction removal efficiencies (DREs). Oxygen and hydroxyl radicals generated in the plasma at a low temperature (293 K) can be used to oxidize hydrocarbons to CO, CO_2 and H_2O. Near complete destruction of C_6H_6 (>99%) was achieved [4]. Oxygen can be used to help decompose C_6H_6 in the radio-frequency (RF) plasma. This concept was employed by Tezuka et al. to identify the conversion efficiency from C_6H_6 to phenol [2].

RF plasma was a branch of non-equilibrium plasma, which was frequently termed cold plasma [7]. The kinetic energy of electrons and ions exceeds that of molecules in cold plasma systems. Generally, the temperature of the gas molecule in an RF plasma reactor is near room temperature, while that of electrons in the plasma zone could exceed 10^3 K [8], depending on the power input and gas species produced. Following the plasma zone, the temperature of the gas molecules was rapidly quenched to below 400 °C [9]. At such high temperature in the plasma zone, the energy of an electron is around 50 kcal/mol, which is twice that of the activation energy of a conventional chemical reaction (25 kcal/mol). Accordingly, conventional reactions, which must be performed at very high temperatures could be completed at lower temperatures in

* Corresponding author. Tel.: +886 6 275 7575x65829; fax: +886 6 275 2790.
E-mail address: tachang@mail.ncku.edu.tw (T.-C. Lin).

0304-3894/$ – see front matter © 2004 Elsevier B.V. All rights reserved.
doi:10.1016/j.jhazmat.2004.09.006

the RF plasma reactor. Due to the advantage of low operating temperature and high decomposition efficiency, the RF plasma technology can be considered a potential alternative method for treating VOC.

However, when the plasma technology is applied to treat VOC, the problems of by-products indicated by Demidiouk et al. [10] may be encountered. These by-products contain CO, aerosol and polymer. Applying plasma for removing aromatic organic compounds may be difficult because of the formation of solid by-products [10]. Generally, in the plasma system with oxygen, the final gaseous products generally simultaneously contain CO_2 and CO. The operational parameters could influence the selectivity of CO_2 and CO. These processes should be adjusted to suppress the formation of CO, since it is toxic.

When C_6H_6 is subjected to energetic RF plasma, competition occurs between decomposition and synthesis. From the perspective of mass conservation, C_6H_6 can be decomposed to yield gaseous products, such as H_2, CH_4, C_2H_2, C_2H_4 and C_2H_6, or can be synthesized to produce larger aromatics, for example PAHs and soot. Furthermore, C_6H_6 can be pyrolyzed to carbon black [11,12] or synthesized to larger aromatics (fullerenes) [13] under suitable conditions.

The primary objective of this study is to examine the formation and mechanism of gaseous products during the decomposition of C_6H_6 gas in the RF plasma. The property of solid depositions was also studied.

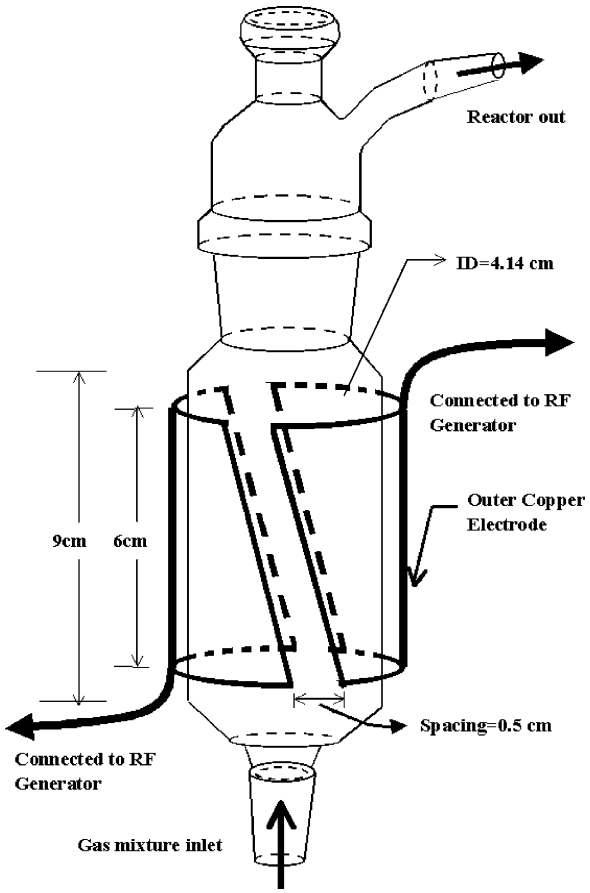

Fig. 1. Plasma reactor.

2. Experimental

Similar experimental apparatus of plasma system has been described in more detail elsewhere [14]. By applying a vacuum, C_6H_6 can be easily transformed into the vapor phase. The flow rates of C_6H_6 gas, H_2, O_2 and argon were individually metered with calibrated mass flow controllers (Brooks-type 5850E). A total flow rate of 100 sccm (cm^3/min, 1 atm, 273 K) entered the mixing vessel and was then introduced into a glass reactor. The operational pressure was always adjusted around 10 Torr before the application of RF plasma. The RF plasma reactor, as illustrated in Fig. 1, is a cylindrical glass vessel, with inner diameter 4.14 cm and total height 20 cm. The outer copper electrode has a height of 6 cm and is wrapped on the plasma reactor and grounded. To achieve steady RF power, the spacing between two electrode sheets was 0.5 cm.

An RF plasma generator (CESAR, Dressler) and a matching network (Dressler, Vario Match) supplied 13.56 MHz power to the reactor. Gas was introduced to the bottom of the reactor flows via glass tubes running into the powered electrode, where it then mixed before flowing into the copper electrode zone. This arrangement ensures that all gas introduced into the reactor flowed through the glow discharge. Before each run, the system was subjected to a vacuum to reduce the pressure to below 0.01 Torr. An oil diffusion pump was then used to further lower the pressure to 0.001 Torr.

The temperature of the electrons in the plasma zone could exceed 10^3 K, depending on the power input and gas species produced. After plasma zone, the gas flow temperature was rapidly quenched to below 400 °C. This study calculated the electron temperature in the plasma zone using the computer model; they were 2220, 2280, 2340, 2400 and 2450 °C for 5, 10, 20, 40 and 60 W, respectively. However, outside the plasma zone, the temperatures at the exit of the plasma reactor were between 200 and 400 °C, depending on power input. Additionally, the temperatures at the filter for collecting particle-phase PAHs were 57 and 115 °C using the input power of 40 and 90 W, respectively. The gaseous product species outside the reactor is on-line introduced into a Fourier transform infrared (FT-IR) spectrometer (Nicolet, Avatar 360) with 9.6 m path length gas cell (CIC, Ranger) for species identification and quantification. Calibration for gaseous reactants and product species was conducted by withdrawing unreacted gases and going directly through the sampling line connected to the FT-IR. The species concentrations were calculated by comparing the response factor (absorbance height/concentration) of standard gas at the same FT-IR wavenumber. Table 1 lists the wavenumber of both the absorbance-zone range and absorbance-peak center for C_6H_6, CH_4, C_2H_2, C_2H_4, C_2H_6, CO and CO_2.

Table 1
The FTIR wave number of absorbance-zone range and absorbance-peak center for seven species

Compound	Formula	Wave number of absorbance-peak center (cm^{-1})	Wave number of absorbance-zone range (cm^{-1})
Benzene	C_6H_6	673	3020–3070, 3080–3120
Methane	CH_4	1304, 1342, 2916, 3012, 3087	1173–1396, 2825–3174
Acetylene	C_2H_2	729, 746, 1297, 1350, 3259, 3306	607–833, 1205–1432, 3159–3371
Ethylene	C_2H_4	950, 1965, 1886, 1910, 3074, 3130	807–1162, 1800–1960, 2883–3285
Ethane	C_2H_6	829, 1436, 1470, 2966, 2985	719–938, 1331–1631, 2573–3321
Carbon monoxide	CO	2117, 2167	1970–2230
Carbon dioxide	CO_2	2332, 2355, 3595, 3629, 3701, 3724	2230–2400, 3500–3750

A steady-state was considered to be attained when a relatively constant value of both decomposition fractions and absorbance-peaks of product species on FT-IR was obtained at designed operational parameters, including gas feed concentration, operational pressures (10 Torr), total gas flow rate (100 sccm) and input power. Each experimental run lasted for at least for 15 min, and the effluent concentration of individual species was monitored by the FT-IR throughout the reaction. In all of the experiments, the analytical results show that the steady-state conditions were approached in the effluent after roughly 10 min. Notably, the data reported here are based on the mean values measured after a steady-state condition was achieved.

3. Results and discussion

3.1. In C_6H_6/Ar plasma

The decomposition fraction of C_6H_6 ($\eta_{C_6H_6}$, %) in the RF plasma system is defined as: [(influent $C_{C_6H_6}$ − effluent $C_{C_6H_6}$)/influent $C_{C_6H_6}$] × 100%, where $C_{C_6H_6}$: C_6H_6 feed concentration. As shown in Fig. 2, at the lower $C_{C_6H_6}$ (0.4%), lower input power (5 W) could have $\eta_{C_6H_6}$ of up to 98%, increasing the input power to 10 W can thoroughly destroy C_6H_6 ($\eta_{C_6H_6}$ = 99%). On the other hand, at the higher $C_{C_6H_6}$ (1.5%), lower input power (5 W) could have $\eta_{C_6H_6}$ of just 80%, in which case increasing input power to 20 W could result in $\eta_{C_6H_6}$ of 99%. From Fig. 2, at the lower input power (5–20 W), C_6H_6 can be easily decomposed at lower $C_{C_6H_6}$, and the $\eta_{C_6H_6}$ increases with increasing input power as observed previously. When input power exceeded 20 W, the $\eta_{C_6H_6}$ can reach 99% at the $C_{C_6H_6}$ of 0.4–1.5%. The above results implied that higher $C_{C_6H_6}$ diluted the power supplied and reduced the $\eta_{C_6H_6}$. However, a higher input power generates more energetic electrons thus promoting the reaction and increasing $\eta_{C_6H_6}$.

Fig. 3 shows the gaseous products during the decomposition of C_6H_6. Under the specified $C_{C_6H_6}$ (0.4–1.5%) and RF power (5–60 W), acetylene (C_2H_2) is the sole gaseous product. This phenomenon results from the C_2H_2 being more stable than other hydrocarbons. Regarding the influence of input power on the formation of C_2H_2, it exhibits good agreement with the results of Ogata et al., where C_2H_2 concentration decreased with increasing input power [5]. When the input power is raised to 20 W, the total carbon input converted into C_2H_2 could be negligible. Regarding the influence of $C_{C_6H_6}$, its formation increases markedly with increasing $C_{C_6H_6}$ when the input power was below 20 W. Based on the experimental results obtained for the plasma by Ogata et al., a small amount

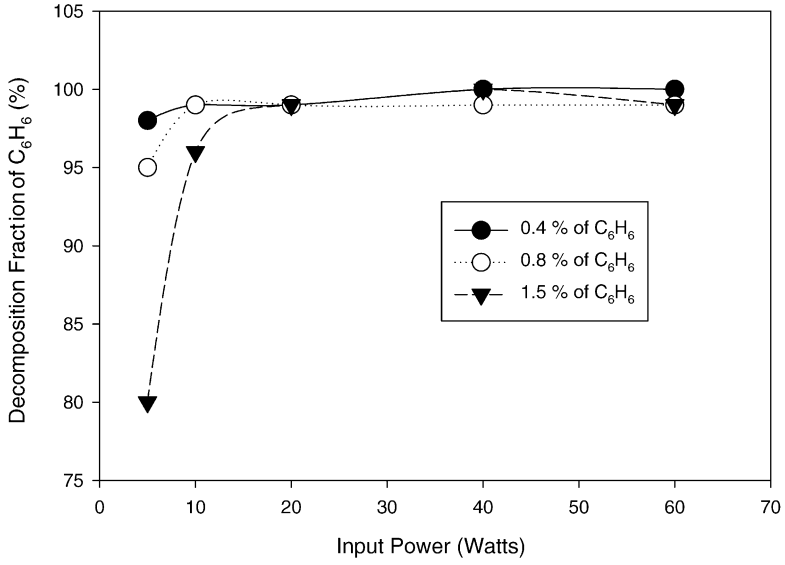

Fig. 2. Decomposition fraction of C_6H_6 with various input power at different feed concentration of C_6H_6 in the C_6H_6/Ar plasma environment.

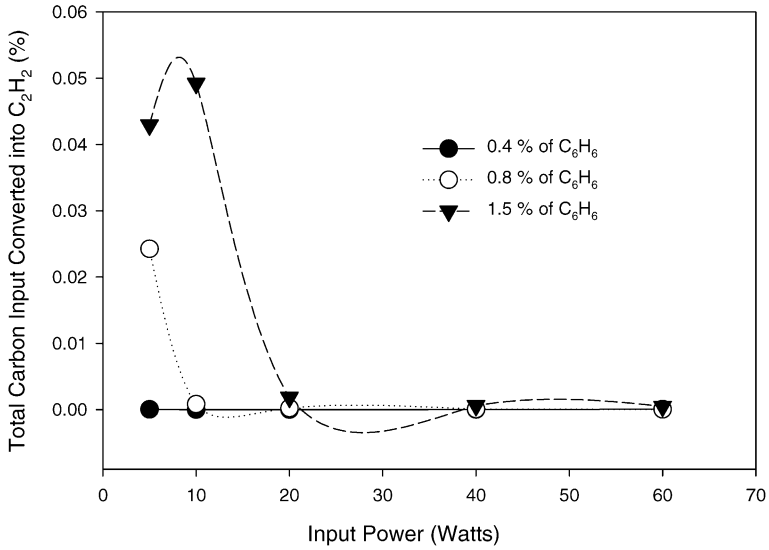

Fig. 3. Total carbon input converted into C_2H_2 ($Y_{C_2H_2}$) with various RF plasma input power at different feed concentration of C_6H_6 in the C_6H_6/Ar system.

of C_2H_2 (7–20 ppm) was detected [1]. Although the participation of catalyst-like factors, such as oxygen or water, could cause further decomposition of C_2H_2 and consequently lower production, low $C_{C_6H_6}$ (200 ppm, equal to 0.02%) could be the main reason for low production in their study. Instead, abundant C_2H_2 (Fig. 3) were found in this study owing to feeding of approximately 20 times of $C_{C_6H_6}$ (0.4–1.5%).

Numerous researchers reported that C_2H_2 was produced from C_6H_6 [1,5,11,15,16]. The production routes included pyrolysis, oxidation, combustion, sonication and plasma. Such information on C_2H_2 formation revealed that C_2H_2 can easily be generated from C_6H_6. From the thermodynamic analysis of C_6H_6 pyrolysis by Cataldo [16], acetylene formation from C_6H_6 ($C_6H_6 \rightarrow 3C_2H_2$) is possible only if C_6H_6 is pyrolyzed at very high temperature (1700 °C). Since it is difficult to imagine that such high temperature is reached during C_6H_6 decomposition in the RF plasma, the alternative explanation is that acetylene is formed along with 'coke' via the following reaction: $C_6H_6 \rightarrow C_2H_2 + 4C\,(coke) + 2H_2$. Meanwhile, naphthalene and other PAHs can be formed if 'coke' formation occurs. $2C_6H_6 \rightarrow C_{10}H_8$ (naphthalene) + 2C (coke) + $4H_2$. In fact, based on the results of this study, simultaneous formation of PAHs (polycyclic aromatic hydrocarbons) and dark yellow-to-brown matter was found upon prolonged decomposition of C_6H_6 [17]. Although abundant electrons with high energy are generated in the energetic RF plasma environment for introducing reactions, the temperature of the bulk environment of gaseous products remains low. Consequently, decomposition of C_6H_6 to the sole product, acetylene (C_2H_2), is impossible. Instead, other products, such as solid depositions, PAHs and H_2 must be formed simultaneously through the following two reactions [16]:

$$C_6H_6 \rightarrow C_2H_2 + 4C(coke) + 2H_2$$

$$2C_6H_6 \rightarrow C_{10}H_8(naphthalene) + C_2H_2 + H_2$$

3.2. *In C_6H_6/H_2/Ar plasma*

As shown in Fig. 4, at a lower input power (Fig. 4(A), 20 W), decomposition of C_6H_6 at a lower $C_{C_6H_6}$ (1%) is not considerably influenced by increasing the H_2/C_6H_6 ratio. The $\eta_{C_6H_6}$ exceeded 98%. Moreover, for a higher $C_{C_6H_6}$ (1.5%), the $\eta_{C_6H_6}$ decreased with increasing H_2/C_6H_6 ratio. At a higher input power (Fig. 4(B), 40 W), the trends of $\eta_{C_6H_6}$ closely resembled those in Fig. 4(A) for both 1 and 1.5% of $C_{C_6H_6}$. Comparing Fig. 4(A) and (B), at lower $C_{C_6H_6}$ (1%) no obvious difference was identified between the trends of $\eta_{C_6H_6}$ when input power was raised from 20 to 40 W; whereas, at a higher $C_{C_6H_6}$ (1.5%), despite the trends of $\eta_{C_6H_6}$ being similar, a higher input power can be seen to result in a higher $\eta_{C_6H_6}$. Regarding the influence of $C_{C_6H_6}$ on its $\eta_{C_6H_6}$, as indicated in the previous section, a lower $C_{C_6H_6}$ (1%) created a higher $\eta_{C_6H_6}$ for Fig. 4(A) and (B), respectively. The decomposition of C_6H_6 is related to the reaction of H-abstraction. Thus, H_2 addition hindered the reaction of H-abstraction, then decreasing the $\eta_{C_6H_6}$. On the other hand, increasing $C_{C_6H_6}$ decreased $\eta_{C_6H_6}$. $\eta_{C_6H_6}$ decreased because the power applied on each C_6H_6 molecule reduced with increasing number of C_6H_6 molecules being fed. It can be summarized that the operational conditions for obtaining an improved $\eta_{C_6H_6}$ in the C_6H_6/H_2/Ar plasma would be low $C_{C_6H_6}$, high input power and low H_2/C_6H_6 ratio.

Regarding the formation of gaseous products, besides C_2H_2, this study also found that CH_4, C_2H_4 and C_2H_6 were obtained in the C_6H_6/H_2/Ar plasma (Fig. 5(A) and (B)). As to the molecular structures, the H/C ratio (molar ratio) of CH_4, C_2H_4 and C_2H_6 each exceeded that of C_2H_2, which was the sole species in the C_6H_6/Ar system, meaning that addition of hydrogen can enhance the formation of hydrogen-rich species. Furthermore, as illustrated in Fig. 5(A) and (B), high H/C ratio species (CH_4 and C_2H_6) dominated relatively low H/C ratio species (C_2H_2 and C_2H_4). Generally, the total

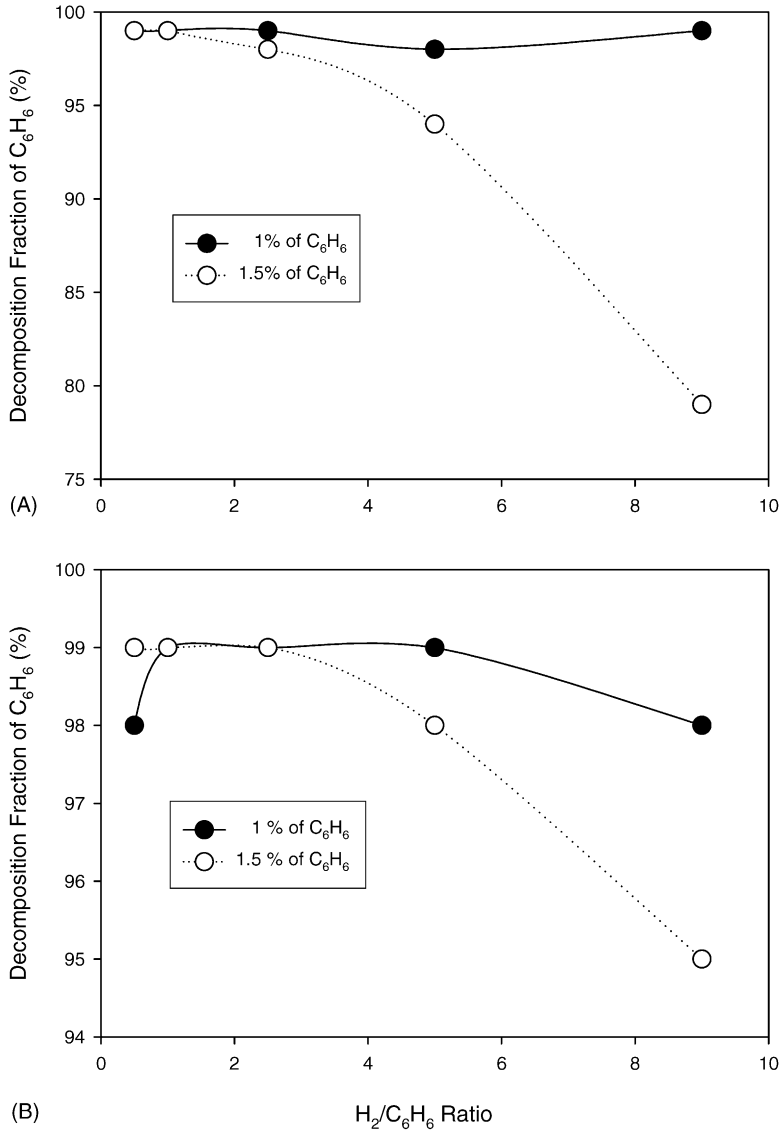

Fig. 4. Decomposition fraction of C_6H_6 with various H_2/C_6H_6 ratio at different feed concentration of C_6H_6 and RF plasma input power, (A) for 20 W and (B) for 40 W.

carbon input converted into gaseous products (Y_{gas}) increased with increasing H_2/C_6H_6 ratio. Moreover, the growing speed with various H_2/C_6H_6 ratios for CH_4 and C_2H_6 also exceeded that for C_2H_2 and C_2H_4. All the above results revealed and strengthened the fact that hydrogen addition favors the formation of hydrogen-rich species.

As described in the previous section on the gaseous products (Fig. 3), 20 W of input power can make the $Y_{C_2H_2}$ negligible in the C_6H_6/Ar system, where C_2H_2 is the sole gaseous product. That is, input power exceeding 20 W could completely destroy all the organics at $C_{C_6H_6}$ below 1.5%. However, this study still found significant amounts of CH_4, C_2H_2, C_2H_4 and C_2H_6 in Fig. 5, where $C_{C_6H_6}$ was 1.5% and the input power was at least 20 W. The possible reason for the above results was that the addition of hydrogen activated these 'carbon depositions', then reacted with activated carbons to produce stable hydrocarbons and even hydrogen-rich species in the energetic plasma.

In Fig. 5, C_2H_6 denotes the most abundant hydrogen-rich hydrocarbon species. The trend of $Y_{C_2H_6}$ resembles those of CH_4, C_2H_2 and C_2H_4, respectively, which increased with increasing H_2/C_6H_6 ratio. Comparing Fig. 5(A) and (B), based on the same H_2/C_6H_6 ratio, found that $Y_{C_2H_6}$ reduced with increasing input power. High amount of C_2H_6 formation probably results from the combination of two methyl radical ($CH_3^{\bullet}$), which frequently occurs in the plasma environment since CH_4 is also a dominant species following hydrogen addition.

Due to predictions of a future oil shortage, this study mentions that these final gas products (including CH_4, C_2H_2, C_2H_4 and C_2H_6) formed in the C_6H_6/Ar and C_6H_6/H_2/Ar RF plasma systems are worthy of recovery and reuse, and could provide useful alternatives to existing fuels.

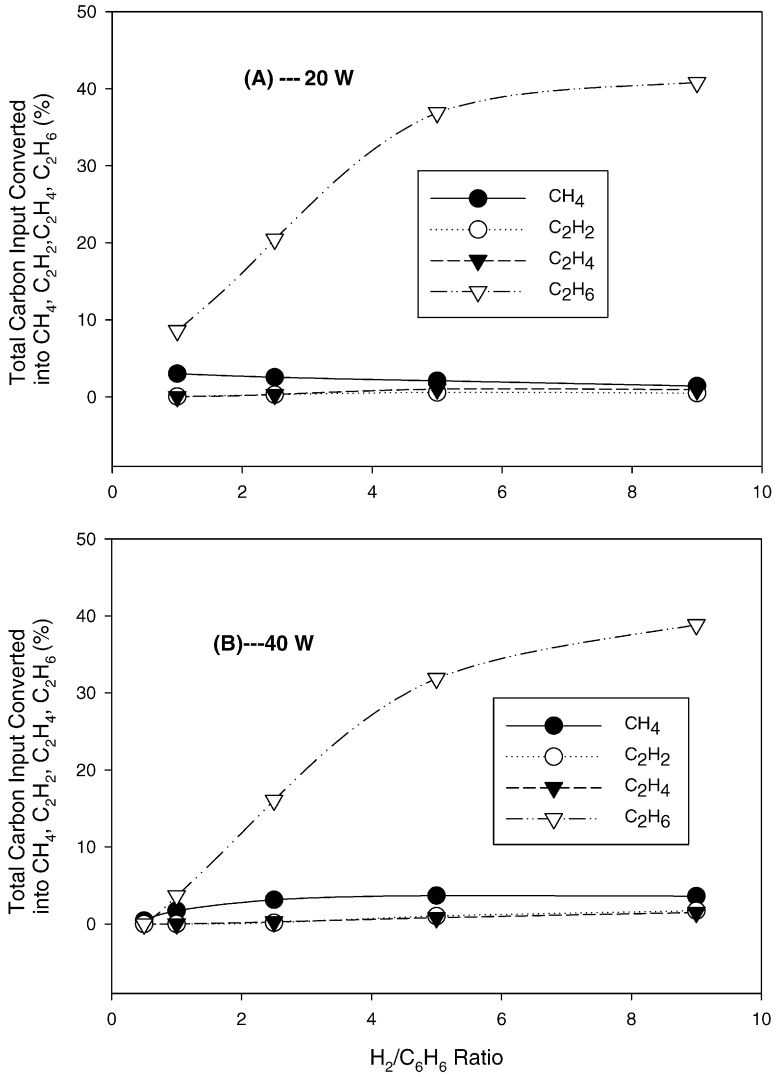

Fig. 5. Total carbon input converted into the major gaseous products with various H_2/C_6H_6 ratio during the decomposition of 1.5% of C_6H_6 in the $C_6H_6/H_2/Ar$ system, (A) for 20 W and (B) for 40 W.

3.3. In $C_6H_6/O_2/Ar$ plasma

Fig. 6 clearly shows that, at the input power of 20 W, increasing the O_2/C_6H_6 ratio from 1.0 to 9.0 (1–9% O_2) does not significantly influence the $\eta_{C_6H_6}$ at $C_{C_6H_6}$ of 1%, and $\eta_{C_6H_6}$s maintained at 98–99%. This information implies that C_6H_6 with $C_{C_6H_6}$ of 1% can be completely oxidized at input power of 20 W and O_2/C_6H_6 ratio of 1.0. The final products in the $C_6H_6/O_2/Ar$ plasma are CO_2, CO and H_2O. This study cannot find other gaseous products, even phenol, which are frequently found in the combustion process and plasma system with oxygen. This finding displayed good agreement with the results of Kim et al. [18], where decomposed C_6H_6 was mostly converted to CO_2 and CO, and no other organic reaction products were detected from the gas analysis using FT-IR. Regarding combustion, the stoichiometric oxygen for 1% of C_6H_6 was 7.5%. In this RF plasma system, 1% of oxygen at the lower input power of 20 W can achieve the complete decomposition, exhibiting the advantage of this system over the conventional combustion system.

Fig. 7 shows the formation of gaseous products associated with carbon (CO_2 and CO) and carbon depositions in the $C_6H_6/O_2/Ar$ system. When O_2/C_6H_6 ratio were increased, the Y_{CO_2} maintains a constant value of 22%, while the Y_{CO} decreases with increasing O_2/C_6H_6 ratio until the stoichiometric point ($O_2/C_6H_6 = 7.5$) is reached. Subsequently, Y_{CO} displayed the opposite trend. Thus, the trend for the formation of carbon depositions exhibited the opposite direction to CO.

Fig. 7 clearly shows that Y_{CO_2} always exceed Y_{CO} for all O_2/C_6H_6 ratios. This result differs from that of Demidiouk et al. [10], where plasma treatment without catalyst increases total gas toxicity due to more toxic CO being formed (the removal efficiency for toluene was 97%, and that for C_6H_6 was 98–99% in this study). Generally, in the combustion process or plasma system with oxygen, the final gaseous products

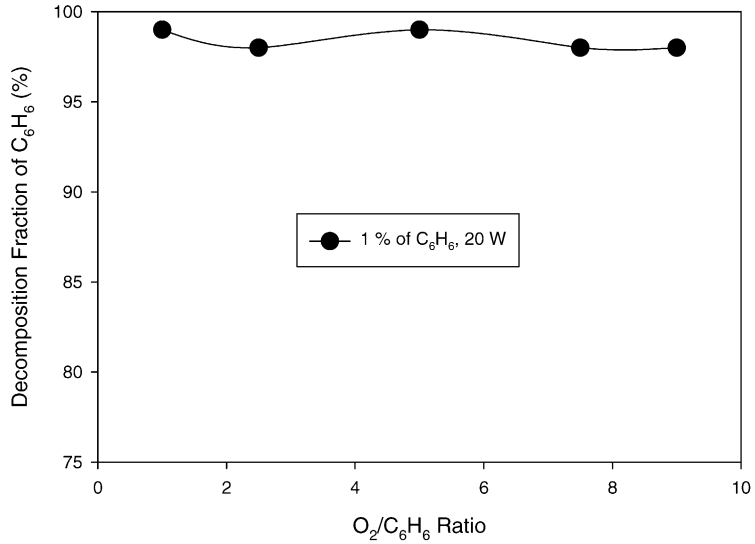

Fig. 6. Decomposition fraction of C_6H_6 with various O_2/C_6H_6 ratio at 1% of C_6H_6 feed concentration and 20 W of input power in the C_6H_6/O_2/Ar system.

simultaneously contain CO_2 and CO. The better selection for operational parameters or environments decreases the Y_{CO}, and decreases the toxicity accordingly. Furthermore, adding the catalysts following plasma reactor could provide the best means of solving the toxicity problem from CO.

3.4. Formation of solid depositions

Examining the gaseous products generated from C_6H_6/Ar, C_6H_6/H_2/Ar and C_6H_6/O_2/Ar plasmas described above, the total carbon mass on gaseous product was found to be markedly lower than that of input C_6H_6. Therefore, a significant amount of carbon input was being converted into solid depositions. In accordance with the study results, which are also submitted in part II, a significant amount of PAHs were detected in this RF plasma system [17]. Based on the concept of carbon balance, the fraction of total carbon input converted into carbon depositions was depicted in Fig. 8((A) for the C_6H_6/Ar system and (B) for the C_6H_6/H_2/Ar system) and Fig. 7 (C_6H_6/O_2/Ar system, as previously illustrated). Evidently, from these three illustrations, carbon depositions account for the majority of the decomposed C_6H_6, particularly for the C_6H_6/Ar system, where almost all the decomposed C_6H_6 were converted into carbon depositions (Fig. 8(A) closely resembled Fig. 2). In the C_6H_6/H_2/Ar system, because of the addition of H_2, parts of carbon reacted with them to produce gaseous hydrocarbons, then carbon depositions decreased with increasing H_2/C_6H_6 ratio. In the C_6H_6/O_2/Ar

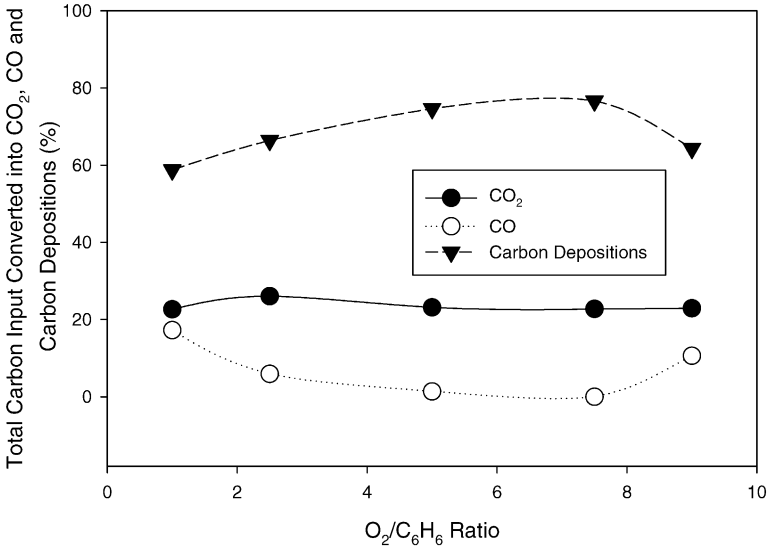

Fig. 7. Total carbon input converted into CO_2, CO and carbon depositions with various O_2/C_6H_6 ratio in the C_6H_6/O_2/Ar system (1% of C_6H_6 and 20 W of input power).

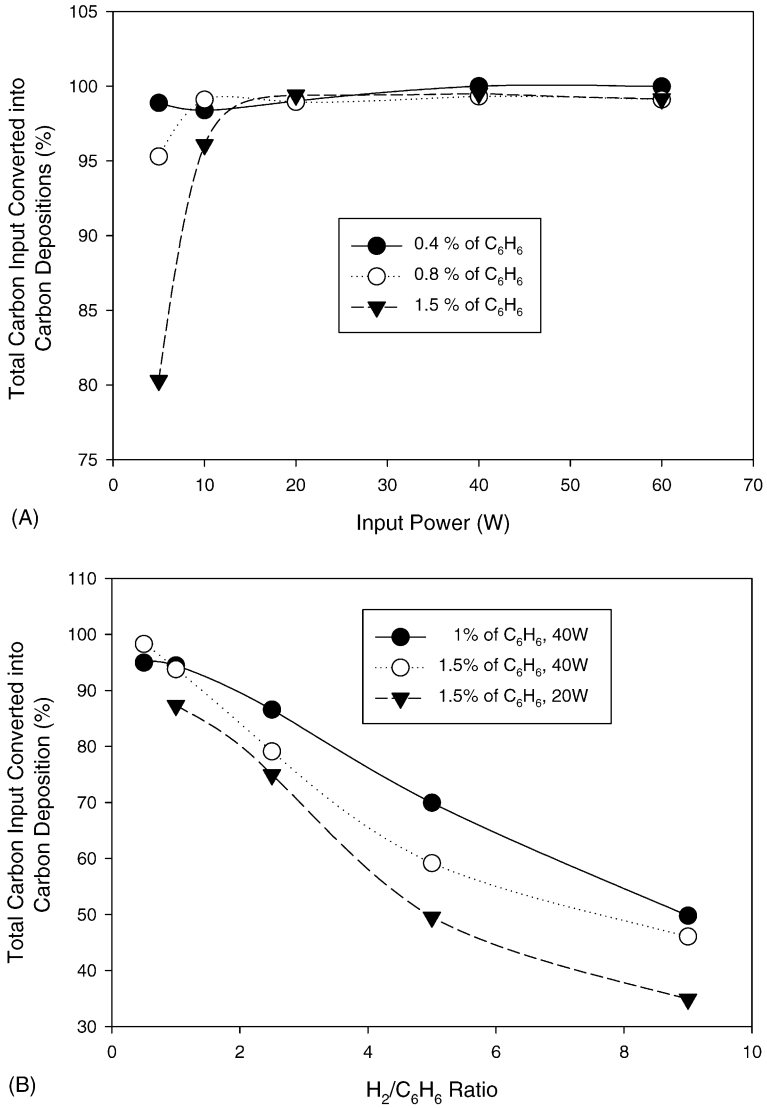

Fig. 8. The carbon depositions during the decomposition of C_6H_6 in both the C_6H_6/Ar (A) and C_6H_6/H_2/Ar (B) systems.

system, the addition of O_2 resulted in the formation of the relatively stable species, CO_2 and CO, in which case the amount of carbon depositions was less than for the C_6H_6/Ar system.

The solid depositions on the internal wall of plasma reactor were collected and analyzed by ESCA (electron spectroscopy for chemical analysis). Two sets of operational parameters were chosen: 10% C_6H_6, 40 W for C_6H_6/Ar system and 2% C_6H_6, 40 W, 1% O_2 for C_6H_6/O_2/Ar system. Fig. 9 shows that the fraction of total carbon input converted into solid depositions (Y_{solid}) accounts for 99.77% in the C_6H_6/Ar system (Fig. 9(A)) and 99.18% (besides 0.82% of O_2) in the C_6H_6/O_2/Ar system (Fig. 9(B)). Peak deconvolution (using Gaussian model) of the carbon spectra was carried out for determining the functional components of the solid deposition. The analytical results show the possible existence of C–C bond (binding energy: 285.65 eV) and C–H bond (binding energy: 286.45 eV) [19–22], and the ratio of C–C bond to C–H bond is approximately 1.4 to 1; whereas, in the C_6H_6/O_2/Ar system, the binding energy for C–C and C–H bond was 285.6 and 286.7 eV, respectively, [19–22], and the ratio was 6.3 to 1.0.

Additionally, element analysis was also conducted at two specified operational conditions: 10% C_6H_6, 40 W and 2% C_6H_6, 40 W, 15% O_2. In solid deposition, the relative percentages of carbon/hydrogen content were 89.51%/6.57% and 85.53%/6.71%, which represented ratios of 13.6:1 and 12.7:1, respectively. That is, the molar ratios were 1.14 and 1.06, respectively. The above results revealed that carbon depositions account for the major parts of total carbon mass in both C_6H_6/Ar and C_6H_6/O_2/Ar systems. This result demonstrates good agreement with the results of XPS (ESCA) mentioned previously.

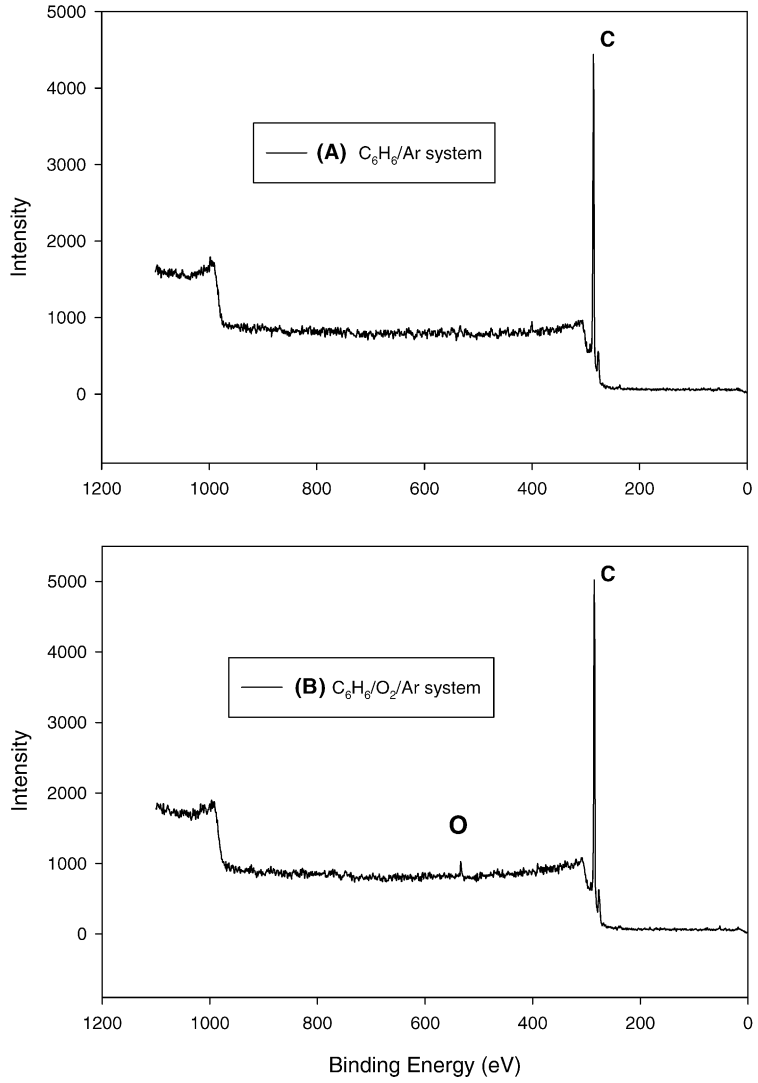

Fig. 9. The ESCA spectrum between C_6H_6/Ar (10% of C_6H_6, 40 W) and C_6H_6/O_2/Ar (2% of C_6H_6, 40 W, 1% of O_2) system.

The carbon content in solid depositions is the most significant influence on their heat value. The heat value of 7000 kcal/kg for the operational condition of 10% C_6H_6 and 90 W significantly exceeded that of plastics (4000–5000 kcal/kg). Comparing the findings of this study with Table 2, which lists the carbon content and heat value of various coal [23], these 'carbon depositions' could be categorized into the rank between Anthracite and Bituminous. Besides being the alternative fuel, these solid by-products should be controlled by employing air pollutant control devices, such as bag house.

Table 2
Carbon content and heat value of various coal [23]

Ranks of coal	Carbon content (%)	Heat value, BTU/pound (kcal/kg)
Anthracite	86–98	15000 (8328)
Bituminous	45–86	10500–15500 (5830–8606)
Subbituminous	35–45	8300–13000 (4608–7218)
Lignite	25–35	4000–8300 (2221–4608)

4. Conclusions

(1) In the C_6H_6/Ar RF plasma system and at lower input power (5–20 W), C_6H_6 can be decomposed more easily at lower input concentration (0.4–1.5%), and $\eta_{C_6H_6}$ increased with increasing input power; while at a higher input power (above 20 W), $\eta_{C_6H_6}$ can reach up to 99% at 0.4–1.5% of $C_{C_6H_6}$. Acetylene (C_2H_2) is the only significant gaseous-product being detected in the C_6H_6/Ar RF plasma system. The fraction of total carbon input converted into C_2H_2 ($Y_{C_2H_2}$) decreased with increasing input power.

(2) In the C_6H_6/H_2/Ar system, lower $C_{C_6H_6}$, high input power, and lower H_2/C_6H_6 ratio could lead to better decomposition of C_6H_6. Addition of hydrogen could help in forming hydrogen-rich species like CH_4, C_2H_4 and C_2H_6.

(3) In the C_6H_6/O_2/Ar system, the C_6H_6 with 1% of feed concentration mixed with 1% of O_2 can be totally

decomposed at input power of 20 W. The stable products were CO_2, CO and H_2O and no measurable phenol was found.

(4) The total carbon mass on the gaseous product was considerably lower than that of input C_6H_6. Consequently, a significant quantity of carbon input was converted into solid depositions among C_6H_6/Ar, C_6H_6/H_2/Ar and C_6H_6/O_2/Ar systems. Most carbon contents (carbon depositions) were deposited on the reactor internal wall. Particularly for the C_6H_6/Ar system, very little C_6H_6 was pyrolyzed to C_2H_2. In the C_6H_6/H_2/Ar plasma, carbon partially reacted with H_2 to produce hydrogen-rich species, such as CH_4, C_2H_4 and C_2H_6.

(5) The results of ESCA, element analysis, and heat value analysis show that high carbon contents of carbon depositions result in heat values up to 7000 kcal/kg, and these 'carbon depositions' could be categorized into the rank between Anthracite and Bituminous.

References

[1] A. Ogata, K. Yamanouchi, K. Mizuno, S. Kushiyama, T. Yamamoto, Oxidation of dilute benzene in an alumina hybrid plasma reactor at atmospheric pressure, Plasma Chem. Plasma Process. 19 (1999) 383–394.

[2] M. Tezuka, T. Yajima, Oxidation of aromatic hydrocarbons with oxygen in a radiofrequency plasma, Plasma Chem. Plasma Process. 16 (1996) 329–340.

[3] D.L. McCorkle, W. Ding, C.Y. Ma, L.A. Pinnaduwage, Dissociation of benzene in a pulsed glow discharge, J. Appl. Phys. 86 (7) (1999) 3550–3557.

[4] M.P. Cal, M. Schluep, Destruction of benzene with non-thermal plasma in dielectric barrier discharge reactors, Environ. Prog. 20 (2001) 151–156.

[5] A. Ogata, N. Shintani, K. Yamanouchi, K. Mizuno, S. Kushiyama, T. Yamamoto, Effect of water vapor on benzene decomposition using a non-thermal-discharge plasma reactor, Plasma Chem. Plasma Process. 20 (4) (2000) 453–467.

[6] H. Sekiguchi, Catalysis assisted plasma decomposition of benzene using dielectric barrier discharge, Can. J. Chem. Eng. 79 (Aug.) (2001) 512–516.

[7] B. Eliasson, U. Kogelschatz, Nonequilibrium volume plasma chemical processing, IEEE Trans. Plasma Sci. 19 (1991) 1063–1077.

[8] L.T. Hsieh, W.J. Lee, C.Y. Chen, M.B. Chang, H.C. Chang, Converting methane by using an RF plasma reactor, Plasma Chem. Plasma Process. 18 (1998) 215–239.

[9] W.T. Liao, W.J. Lee, C.Y. Chen, M. Shih, Decomposition of ethylene oxide in the RF plasma environment, Environ. Technol. 22 (2001) 165–173.

[10] V. Demidiouk, S.I. Moon, J.O. Chae, Toluene butyl acetate removal from air by plasma-catalytic system, Catal. Commun. 4 (2003) 51–56.

[11] R.S. Slysh, C.R. Kinney, Some kinetics of the carbonization of benzene, acetylene and diacetylene at 1200°C, J. Phys. Chem. 65 (1961) 1044–1045.

[12] J.R. Fincke, R.P. Anderson, T.A. Hyde, B.A. Detering, Plasma pyrolysis of methane to hydrogen and carbon black, Ind. Eng. Chem. Res. 41 (2002) 1425–1435.

[13] H. Richter, W.J. Grieco, J.B. Howard, Formation mechanism of polycyclic aromatic hydrocarbons and fullerenes in premixed benzene flames, Combust. Flame 119 (1999) 1–22.

[14] M. Shih, W.J. Lee, C.H. Tsai, Decomposition of SF_6 in an RF plasma environment, J. Air Waste Manag. Assoc. 52 (2002) 1274–1280.

[15] C.S. McEnally, L.D. Pfefferle, The effects of slight premixing on fuel decomposition and hydrocarbon growth in benzene-doped methane nonpremixed flames, Combust. Flame 129 (2002) 305–323.

[16] F. Cataldo, Ultrasound-induced cracking and pyrolysis of some aromatic and naphthenic hydrocarbons, Ultrason. Sonochem. 7 (2000) 35–43.

[17] S.I. Shih, T.C. Lin, M. Shih, Decomposition of benzene in the RF plasma environment part II: formation of polycyclic aromatic hydrocarbons, J. Hazard. Mater., submitted for publication.

[18] H.H. Kim, Y.H. Lee, A. Ogata, S. Futamura, Plasma-driven catalyst processing packed with photocatalyst for gas-phase benzene decomposition, Catal. Commun. 4 (2003) 347–351.

[19] W.H. Lee, J.Y. Kim, Y.K. Ko, P.J. Reucroft, J.W. Zondlo, Surface analysis of carbon black waste materials from tire residues, Appl. Surf. Sci. 141 (1999) 107–113.

[20] D. Popovici, G. Czeremuzkin, M. Meunier, E. Sacher, Laser-induced metal-organic chemical vapor deposition (MOCVD) of Cu(hfac)(TMVS) on amorphous teflon AF1600: an XPS study of the interface, Appl. Surf. Sci. 126 (1998) 198–204.

[21] W.H. Lee, P.J. Reucroft, Vapor adsorption on coal- and wood-based chemically activated carbons (I) surface oxidation states and adsorption of H_2O, Carbon 37 (1999) 7–14.

[22] D. Fornasiero, F. Li, J. Ralston, R.St.C. Smart, Oxidation of Galena surfaces. 1. X-ray photoelectron spectroscopic and dissolution kinetics studies, J. Colloid Int. Sci. 164 (1994) 333–344.

[23] http://www.ket.org/Trips/Coal/AGSMM/agsmmtypes.html.